SINP/TNP/05-16
hep-ph/0507250

arXiv:hep-ph/0507250v2 19 Jul 2006

Angular distribution of Drell-Yan process at hadron colliders to NLO-QCD in models of TeV scale gravity

Prakash Mathews[a] *, **V. Ravindran**[b] †

a) Saha Institute of Nuclear Physics, 1/AF Bidhan Nagar, Kolkata 700 064, India.

b) Harish-Chandra Research Institute, Chhatnag Road, Jhunsi, Allahabad, India.

ABSTRACT

In TeV scale gravity models, for dilepton production at hadron colliders, we present the NLO-QCD corrections for the double differential cross section in the invariant mass and scattering angle. For both ADD and RS models, the quantitative impact of QCD corrections for extra dimension searches at LHC and Tevatron are investigated. We present the K-factors for both ADD and RS models at LHC and Tevatron. Inclusion of QCD corrections to NLO stabilises the cross section with respect to scale variations.

*prakash.mathews@saha.ac.in
†ravindra@mri.ernet.in

1 Introduction

Extra dimension scenarios are now essential part of the studies of physics beyond the Standard Model (SM). They provide an alternate view of the hierarchy between the electroweak and the Planck scale. Some of these extra dimension models invoke the brane world scenarios to hide the extra spacial dimensions from current observation. Two such models that are phenomenologically widely studied are the Arkani-Hamed, Dimopoulos and Dvali (ADD) [1] and the Randall-Sundrum (RS) [2] models.

In the ADD case the compactified extra dimensions could be large and the large volume of the compactified extra spacial dimension would account for the dilution of gravity in 4-dimensions and hence the hierarchy. In this model, new physics can appear at a mass scale of the order of a TeV. A viable mechanism to hide the extra spacial dimension, is to introduce a 3-brane with negligible tension and localise the SM particles on it. Only the graviton is allowed to propagate the full $4+d$ dimensional space time. As a consequence of these assumptions, it follows from Gauss Law that the effective Planck scale M_P in 4-dimension is related to the $4+d$ dimensional fundamental scale M_S through the volume of the compactified extra dimensions [1]. The extra dimensions are compactified on a torus of common circumference R. The number of extra spacial dimension possible is $d > 2$ from current experimental limits on deviation from inverse square law [3]. The space time is factorisable and the 4-dimensional spectrum consists of the SM confined to 4-dimensions and a tower of Kaluza-Klien (KK) modes of the graviton propagating the full $4+d$ dimensional space time.

The interaction of the KK modes $h_{\mu\nu}^{(\vec{n})}$ with the SM fields localised on the 3-brane is given by

$$\mathcal{L}_{int} \sim -\frac{1}{M_P} \sum_{\vec{n}=0}^{\infty} T^{\mu\nu}(x) h_{\mu\nu}^{(\vec{n})}(x) \,, \tag{1.1}$$

where $T^{\mu\nu}$ is the energy-momentum tensor of the SM fields on the 3-brane. The zero mode corresponds to the usual 4-dimensional massless graviton. The KK modes are all M_P suppressed but the high multiplicity could lead to observable effects at present and future colliders. The Feynman rules are given in [4, 5].

In the RS model there is only one extra spacial dimension and the extra dimension is compactified to a circle of circumference $2L$ and further orbifolded by identifying points related by $y \to -y$. Two branes are placed at orbifold fixed points, $y = 0$ with positive tension called the Planck brane and a second brane at $y = L$ with negative tension called the TeV brane. For a special choice of parameters, it turns out that the 5-dimensional Einstein equations have a warped solution for $0 < y < L$ with metric $g_{\mu\nu}(x^\rho, y) = \exp(-2ky)\ \eta_{\mu\nu}$, $g_{\mu y} = 0$ and $g_{yy} = 1$. This space is not factorisable and has a constant negative curvature— AdS_5 space-time. k is the curvature of the AdS_5 space-time and $\eta_{\mu\nu}$ is the usual 4-dimensional flat Minkowski metric. In this model the mass scales vary with y according to the exponential warp factor. If gravity originates on the brane at $y = 0$, TeV scales can be generated on the brane at $y = L$ for $kL \sim 10$. The apparent hierarchy is generated by the exponential warp factor and no additional large hierarchies appear. The size of the extra dimension is of the order of M_P^{-1}. Further it has been showed that [6] the value of kL can be stabilised without fine tuning by minimising the potential for the modulus field which describes the relative motion of the two branes. In the RS model graviton and the modulus field can propagate the full 5-dimensional space time while the SM is confined to the TeV brane. The 4-dimensional spectrum contains the KK modes, the zero mode is M_P suppressed while the excited modes are massive and are only TeV suppressed. The mass gap of the KK modes is determined by the difference of the successive zeros of the Bessel function $J_1(x)$ and the scale $m_0 = k\ e^{-\pi kL}$. As in the ADD case the phenomenology of the RS model concerns the effect of massive KK modes of the graviton, though the spectrum of the KK mode is quite different.

In the RS model the massive KK modes $h^{(n)}_{\mu\nu}(x)$ interacts with the SM fields

$$\mathcal{L}_{int} \sim -\frac{1}{M_P} T^{\mu\nu}(x) h^{(0)}_{\mu\nu}(x) - \frac{e^{\pi kL}}{M_P} \sum_{n=1}^{\infty} T^{\mu\nu}(x) h^{(n)}_{\mu\nu}(x) \,, \tag{1.2}$$

where $T^{\mu\nu}$ is the energy-momentum tensor of the SM fields on the 3-brane at $y = L$. The masses of $h^{(n)}_{\mu\nu}(x)$ are given by $M_n = x_n \; k \; e^{-\pi kL}$, where x_n are the zeros of the Bessel function $J_1(x)$. In the RS model there are two parameters which are $c_0 = k/M_P$, the effective coupling [‡] and M_1 the mass of the first KK mode. Expect for an overall warp factor the Feynman rule of RS is the same as those of the ADD model.

Next to leading order (NLO) QCD corrections have been recently calculated in the ADD case for $e^+e^- \to$ hadrons [7] and various distributions of invariant lepton pair production at both LHC and Tevatron [8]. This was further extended to the RS case [9]. In this paper, for the ADD and RS models, we consider the un-integrated distribution with respect to $\cos\theta^*$ to NLO in QCD, where θ^* is the scattering angle of the lepton with an initial hadron in the *c.o.m* frame of the lepton pair. This is particularly important in the dilepton production case to achieve maximum sensitivity to the model parameters, as $\cos\theta^*$ integrated cross section is independent of the interference between SM and gravity [8]. To leading order (LO), this double differential $d\sigma/dQ/d\cos\theta^*$ was analysed in [10]. At hadron colliders the NLO-QCD corrections are important especially in models of extra dimension as gluon-gluon subprocess contributes at the same LO as quark-antiquark subprocess. DØ Collaboration recently reported searches for large extra dimensions in the dimuon channel for the double differential cross section [11], this updates the earlier Run-I results [12]. The first direct search of the RS KK modes using the dileptons have been reported by DØ Collaboration [13].

Rest of the paper is organised as follows: In section 2 we evaluate the NLO coefficient functions to the subprocess that contribute to the double differential cross section $d\sigma/dQ/d\cos\theta^*$. Finally in section 3, we discuss the impact of the NLO results.

[‡] An alternate definition is $\bar{c}_0 = k/\overline{M}_P$, where $\overline{M}_P = M_P/\sqrt{8\pi}$, hence $\bar{c}_0 \; = \; c_0 \; \sqrt{8\pi}$.

2 Drell-Yan $\cos\theta^*$ distribution

We consider the Drell-Yan process and study the double differential cross section with respect to the invariant mass of the final lepton pair and $\cos\theta^*$ the cosine of the angle between the final state lepton momenta and the initial state hadron in the $c.o.m$ frame of the lepton pair [§]. The relevant kinematical formulation is detailed in [8]. In the QCD improved parton model, the hadronic cross section can be expressed in terms of partonic cross sections convoluted with appropriate parton distribution functions. The coefficient functions to NLO in QCD are evaluated for both ADD and RS models. The difference between the two models depend on the spectrum of the KK modes and hence summation of the KK modes that contribute to the dilepton production leads to different results [8, 9].

The hadronic part involves the computation of various processes that contribute to Q or X_F or rapidity distributions that are presented in the reference [8]. The angular distributions which are "odd" in $\cos\theta^*$ come mainly from the interferences terms. The non-vanishing odd contribution in the standard model sector comes from the interference of photon mediated processes with Z-boson mediated processes. We also find that non-vanishing odd contributions come from the interference of standard model diagrams with the graviton exchange diagrams. These inference diagrams are absent in the computation of Q, X_F and rapidity distributions where only even functions of $\cos\theta^*$ contribute. We have regularised all the divergences using dimensional regularisation. The mass singularities are removed by the mass factorisation, for details refer to [8].

We first present the angular distribution which is "even" in $\cos\theta^*$.

$$2S\frac{d\sigma_e^{P_1P_2}}{dQ^2 d\cos\theta^*} = \sum_q \mathcal{F}_{SM,q}\int_0^1 dx_1 \int_0^1 dx_2 \int_0^1 dz\, \delta(\tau - z x_1 x_2)$$

[§] An alternate definition of the angle has been considered in [14] to study the lepton helicity distribution in polarised Drell-Yan process.

$$
\times\Bigg[H_{q\bar{q}}(x_1,x_2,\mu_F^2)\Big(\Delta_{q\bar{q}}^{(0),\gamma/Z}(z,Q^2,\mu_F^2)+a_s\Delta_{q\bar{q}}^{(1),\gamma/Z}(z,Q^2,\mu_F^2)\Big)
$$

$$
+H_{qg}(x_1,x_2,\mu_F^2)a_s\Delta_{qg}^{(1),\gamma/Z}(z,\mu_F^2)
$$

$$
+H_{gq}(x_1,x_2,\mu_F^2)a_s\Delta_{gq}^{(1),\gamma/Z}(z,\mu_F^2)\Bigg]
$$

$$
+\sum_q \mathcal{F}_{SMGR,q}\int_0^1 dx_1\int_0^1 dx_2\int_0^1 dz\;\delta(\tau-zx_1x_2)
$$

$$
\times\Bigg[H_{q\bar{q}}(x_1,x_2,\mu_F^2)\Big(\Delta_{q\bar{q}}^{(0),G\gamma/Z}(z,Q^2,\mu_F^2)+a_s\Delta_{q\bar{q}}^{(1),G\gamma/Z}(z,Q^2,\mu_F^2)\Big)
$$

$$
+H_{qg}(x_1,x_2,\mu_F^2)a_s\Delta_{qg}^{(1),G\gamma/Z}(z,\mu_F^2)
$$

$$
+H_{gq}(x_1,x_2,\mu_F^2)a_s\Delta_{gq}^{(1),G\gamma/Z}(z,\mu_F^2)\Bigg]
$$

$$
+\sum_q \mathcal{F}_{GR}\int_0^1 dx_1\int_0^1 dx_2\int_0^1 dz\;\delta(\tau-zx_1x_2)
$$

$$
\times\Bigg[H_{q\bar{q}}(x_1,x_2,\mu_F^2)\Big(\Delta_{q\bar{q}}^{(0),G}(z,Q^2,\mu_F^2)+a_s\Delta_{q\bar{q}}^{(1),G}(z,Q^2,\mu_F^2)\Big)
$$

$$
+H_{qg}(x_1,x_2,\mu_F^2)a_s\Delta_{qg}^{(1),G}(z,Q^2,\mu_F^2)
$$

$$
+H_{gq}(x_1,x_2,\mu_F^2)a_s\Delta_{gq}^{(1),G}(z,Q^2,\mu_F^2)
$$

$$
+H_{gg}(x_1,x_2,\mu_F^2)\Big(\Delta_{gg}^{(0),G}(z,Q^2,\mu_F^2)+a_s\Delta_{gg}^{(1),G}(z,Q^2,\mu_F^2)\Big)\Bigg],
\tag{2.1}
$$

where $H_{ab}(x_1,x_2,\mu_F^2)$ are the renormalised partonic distributions and $\Delta_{ab}(z,Q^2,\mu_F^2)$ are the coefficient function corresponding to various subprocess cross section to NLO in QCD. The factors $\mathcal{F}_{SM,q},\mathcal{F}_{GR}$ correspond to pure SM and gravity (GR) part respectively and are given in [8], the factor that corresponds to the interference of

SM and gravity is

$$\mathcal{F}_{SMGR,q} = \frac{\alpha\kappa^2 Q^2}{4\pi}|\mathcal{D}(Q^2)|\left[\frac{Q^2(Q^2-M_Z^2)}{((Q^2-M_Z^2)^2+M_Z^2\Gamma_Z^2)\,c_w^2 s_w^2} g_q^A g_e^A\right], \tag{2.2}$$

where α is the fine structure constant, $\kappa = \sqrt{16\pi}/M_P$. The summation of the KK modes leads to $\mathcal{D}(Q^2)$ for ADD and RS case has been given in [8, 9].

The leading order results read

$$\begin{aligned}
\Delta_{q\bar{q}}^{(0),\gamma/Z} &= \frac{2\pi}{N}\delta(1-z)\left[\frac{3}{8}\left(1+\cos^2\theta^*\right)\right], \\
\Delta_{q\bar{q}}^{(0),G\gamma/Z} &= \frac{\pi}{8N}\delta(1-z)\left[-1+3\cos^2\theta^*\right], \\
\Delta_{q\bar{q}}^{(0),G} &= \frac{\pi}{8N}\delta(1-z)\left[\frac{5}{8}(1-3\cos^2\theta^*+4\cos^4\theta^*)\right], \\
\Delta_{gg}^{(0),G} &= \frac{\pi}{2(N^2-1)}\delta(1-z)\left[\frac{5}{8}(1-\cos^4\theta^*)\right],
\end{aligned} \tag{2.3}$$

and the next to leading order results read

$$\begin{aligned}
\Delta_{q\bar{q}}^{(1)\gamma/Z} &= \left(\frac{2\pi}{N}\right) 4\,C_F\Bigg\{\Bigg[\Big(-4+2\zeta(2)\Big)\delta(1-z)+2\frac{1}{(1-z)_+}\ln\left(\frac{Q^2}{\mu_F^2}\right) \\
&\quad +4\left(\frac{\ln(1-z)}{1-z}\right)_+ + \frac{3}{2}\delta(1-z)\ln\left(\frac{Q^2}{\mu_F^2}\right) - (1+z)\ln\left(\frac{Q^2(1-z)^2}{\mu_F^2 z}\right) \\
&\quad -2\frac{\ln(z)}{1-z}\Bigg]\left(\frac{3}{8}(1+\cos^2\theta^*)\right) + \Big[1-z\Big]\frac{3}{8}\Big(1-3\cos^2\theta^*\Big)\Bigg\}, \\
\Delta_{q(\bar{q})g}^{(1)\gamma/Z} &= \left(\frac{2\pi}{N}\right) T_F\Bigg\{\Bigg[-4z\log(z)+2(1-2z+2z^2)\ln\left(\frac{Q^2(1-z)^2}{\mu_F^2 z}\right)-7z^2\Bigg] \\
&\quad \times\left(\frac{3}{8}(1+\cos^2\theta^*)\right)+\left[\frac{15}{8}+\frac{3}{4}z+3z\log(z)\right] \\
&\quad +\left[-\frac{33}{8}+\frac{27}{4}z-3z\log(z)\right]\cos^2\theta^*\Bigg\},
\end{aligned}$$

$$
\begin{aligned}
\Delta^{(1)\gamma/Z}_{gq(\bar{q})} &= \left(\frac{2\pi}{N}\right) T_F \Bigg\{ \Bigg[-4z\log(z) + 2(1-2z+2z^2)\ln\left(\frac{Q^2(1-z)^2}{\mu_F^2 z}\right)\Bigg] \\
&\quad \times \left(\frac{3}{8}(1+\cos^2\theta^*)\right) + \left[\frac{3}{8} - \frac{3}{4}z + \frac{3}{8}z^2 - \frac{3}{2}z\log(z)\right] \\
&\quad + \left[\frac{3}{8} + \frac{45}{4}z - \frac{93}{8}z^2 + \frac{21}{2}z\log(z)\right]\cos^2\theta^* \Bigg\}, \\
\Delta^{(1)G\gamma/Z}_{q\bar{q}} &= \left(\frac{\pi}{8N}\right) C_F \Bigg[\Big(-12 - 12z + \frac{8}{1-z}\Big)\log(z) + \Big(8+8z\Big)\log(1-z) \\
&\quad -16\left(\frac{\log(1-z)}{1-z}\right)_+ + \Big(4 + 4z - \frac{8}{(1-z)_+} - 6\delta(1-z)\Big)\log\left(\frac{Q^2}{\mu_F^2}\right) \\
&\quad -8\zeta(2)\delta(1-z) - 12 + 12z + 18\delta(1-z)\Bigg]\left(1 - 3\cos^2\theta^*\right), \\
\Delta^{(1)G\gamma/Z}_{q(\bar{q})g} &= \left(\frac{\pi}{8N}\right) T_F \Bigg[\Big(-6 + 4z^2\Big)\log(z) + \Big(-4 + 8z - 8z^2\Big)\log(1-z) \\
&\quad + \Big(-2 + 4z - 4z^2\Big)\log\left(\frac{Q^2}{\mu_F^2}\right) - 5 - 2z + 7z^2\Bigg]\left(1 - 3\cos^2\theta^*\right), \\
\Delta^{(1),G\gamma/Z}_{gq(\bar{q})} &= \left(\frac{\pi}{8N}\right) T_F \Bigg[\Big(2 - 28z + 4z^2\Big)\log(z) + \Big(-4 + 8z - 8z^2\Big)\log(1-z) \\
&\quad + \Big(-2 + 4z - 4z^2\Big)\log\left(\frac{Q^2}{\mu_F^2}\right) - 9 - 22z + 31z^2\Bigg]\left(1 - 3\cos^2\theta^*\right), \\
\Delta^{(1)G}_{q\bar{q}} &= \left(\frac{\pi}{8N}\right) C_F \Bigg\{ \Bigg[\Big(\frac{5}{2} + \frac{5}{2}z - \frac{5}{1-z}\Big)\log(z) + \Big(-5 - 5z\Big)\log(1-z) \\
&\quad +10\left(\frac{\log(1-z)}{1-z}\right)_+ + \Big(-\frac{5}{2} - \frac{5}{2}z + \frac{5}{(1-z)_+} + \frac{15}{4}\delta(1-z)\Big) \\
&\quad \times \log\left(\frac{Q^2}{\mu_F^2}\right) + 5\zeta(2)\delta(1-z) - \frac{15}{2} + \frac{10}{3z} + \frac{15}{2}z - \frac{10}{3}z^2
\end{aligned}
$$

$$
\begin{aligned}
&-\frac{25}{2}\delta(1-z)\Big] + \Big[\Big(\frac{45}{2}+\frac{45}{2}z+\frac{15}{1-z}\Big)\log(z)\\
&+\Big(15+15z\Big)\log(1-z) - 30\left(\frac{\log(1-z)}{1-z}\right)_+ + \Big(\frac{15}{2}+\frac{15}{2}z\\
&-\frac{15}{(1-z)_+} - \frac{45}{4}\delta(1-z)\Big)\log\left(\frac{Q^2}{\mu_F^2}\right) - 15\zeta(2)\delta(1-z) + \frac{225}{2}\\
&-\frac{225}{2}z+\frac{75}{2}\delta(1-z)\Big]\cos^2\theta^* \; + \Big[\Big(-40-40z-\frac{20}{1-z}\Big)\log(z)\\
&+\Big(-20-20z\Big)\log(1-z) + 40\left(\frac{\log(1-z)}{1-z}\right)_+ + \Big(-10-10z\\
&+\frac{20}{(1-z)_+} + 15\delta(1-z)\Big)\log\left(\frac{Q^2}{\mu_F^2}\right) + 20\zeta(2)\delta(1-z) - 150\\
&-\frac{10}{3z}+150z+\frac{10}{3}z^2-50\delta(1-z)\Big]\cos^4\theta^*\Big\},
\end{aligned}
$$

$$
\begin{aligned}
\Delta^{(1)G}_{q(\bar{q})g} \;=\; & \frac{\pi}{8N}T_F\Big\{\Big[\Big(\frac{35}{4}-\frac{10}{z}-10z-\frac{5}{2}z^2\Big)\log(z)+\Big(-\frac{35}{2}+\frac{20}{z}+5z+5z^2\Big)\\
&\times\log(1-z)+\Big(-\frac{35}{4}+\frac{10}{z}+\frac{5}{2}z+\frac{5}{2}z^2\Big)\log\left(\frac{Q^2}{\mu_F^2}\right)\\
&-\frac{15}{8}-\frac{15}{2z}+\frac{75}{4}z-\frac{35}{8}z^2\Big] + \Big[\Big(\frac{135}{4}+45z+\frac{15}{2}z^2\Big)\log(z)\\
&+\Big(-\frac{15}{2}+15z-15z^2\Big)\log(1-z)+\Big(-\frac{15}{4}+\frac{15}{2}z-\frac{15}{2}z^2\Big)\log\left(\frac{Q^2}{\mu_F^2}\right)\\
&+\frac{645}{8}-\frac{375}{4}z+\frac{105}{8}z^2\Big]\cos^2\theta^* + \Big[\Big(-65+\frac{10}{z}-35z-10z^2\Big)\log(z)\\
&+\Big(30-\frac{20}{z}-30z+20z^2\Big)\log(1-z)+\Big(15-\frac{10}{z}-15z+10z^2\Big)
\end{aligned}
$$

$$
\begin{aligned}
&\times \log\left(\frac{Q^2}{\mu_F^2}\right) - \frac{205}{2} + \frac{15}{2z} + \frac{215}{2}z - \frac{35}{2}z^2\Big]\cos^4\theta^*\Big\}\,,\\
\Delta_{gq(\bar{q})}^{(1)G} &= \frac{\pi}{8N}T_F\Big\{\Big[\Big(\frac{35}{4} - \frac{10}{z} + \frac{25}{2}z - \frac{5}{2}z^2\Big)\log(z) + \Big(-\frac{35}{2} + \frac{20}{z} + 5z + 5z^2\Big)\\
&\times \log(1-z) + \Big(-\frac{35}{4} + \frac{10}{z} + \frac{5}{2}z + \frac{5}{2}z^2\Big)\log\left(\frac{Q^2}{\mu_F^2}\right)\\
&+\frac{285}{8} - \frac{35}{2z} - \frac{15}{4}z - \frac{75}{8}z^2\Big] + \Big[\Big(-\frac{465}{4} - \frac{345}{2}z + \frac{15}{2}z^2\Big)\log(z)\\
&+\Big(-\frac{15}{2} + 15z - 15z^2\Big)\log(1-z) + \Big(-\frac{15}{4} + \frac{15}{2}z - \frac{15}{2}z^2\Big)\log\left(\frac{Q^2}{\mu_F^2}\right)\\
&-\frac{1695}{8} - \frac{20}{z} + \frac{615}{4}z + \frac{625}{8}z^2\Big]\cos^2\theta^* + \Big[\Big(185 + \frac{10}{z} + 215z - 10z^2\Big)\\
&\times \log(z) + \Big(30 - \frac{20}{z} - 30z + 20z^2\Big)\log(1-z) + \Big(15 - \frac{10}{z}\\
&-15z + 10z^2\Big)\log\left(\frac{Q^2}{\mu_F^2}\right) + \frac{395}{2} + \frac{545}{6z} - \frac{385}{2}z - \frac{605}{6}z^2\Big]\cos^4\theta^*\Big\}\,,\\
\Delta_{gg}^{(1)G} &= \left(\frac{\pi}{2(N^2-1)}\right)\Big\{C_A\Big[\Big(10 - \frac{5}{z} - 5z + 5z^2 - \frac{5}{1-z}\Big)\log(z)\\
&+\Big(-20 + \frac{10}{z} + 10z - 10z^2\Big)\log(1-z) + 10\left(\frac{\log(1-z)}{1-z}\right)_+\\
&+\Big(-10 + \frac{5}{z} + 5z - 5z^2 + \frac{5}{(1-z)_+} + \frac{55}{12}\delta(1-z)\Big)\log\left(\frac{Q^2}{\mu_F^2}\right)\\
&+5\zeta_2\delta(1-z) + \frac{25}{4} - \frac{85}{12z} - \frac{25}{4}z + \frac{85}{12}z^2 - \frac{1015}{72}\delta(1-z)\Big]\\
&+C_A\Big[\Big(-30 - 30z\Big)\log(z) - 60 - \frac{5}{z} + 60z + 5z^2\Big]\cos^2\theta^*
\end{aligned}
$$

$$
\begin{aligned}
&+C_A\Bigg[\Big(40+\frac{5}{z}+55z-5z^2+\frac{5}{1-z}\Big)\log(z)+\Big(20-\frac{10}{z}\\
&-10z+10z^2\Big)\log(1-z)-10\left(\frac{\log(1-z)}{1-z}\right)_+ +\Big(10-\frac{5}{z}-5z\\
&+5z^2-\frac{5}{(1-z)_+}-\frac{55}{12}\delta(1-z)\Big)\log\left(\frac{Q^2}{\mu_F^2}\right)-5\zeta(2)\delta(1-z)\\
&+\frac{255}{4}+\frac{305}{12z}-\frac{255}{4}z-\frac{305}{12}z^2+\frac{1015}{72}\delta(1-z)\Bigg]\cos^4\theta^*\\
&+T_F n_f\Bigg[-\frac{5}{3}\delta(1-z)\log\left(\frac{Q^2}{\mu_F^2}\right)+\frac{175}{36}\delta(1-z)\Bigg]\\
&+T_F n_f\Bigg[\frac{5}{3}\delta(1-z)\log\left(\frac{Q^2}{\mu_F^2}\right)-\frac{175}{36}\delta(1-z)\Bigg]\cos^4\theta^*\Bigg\}, \qquad (2.4)
\end{aligned}
$$

where $C_F=(N^2-1)/2N$, $C_A=N$ and $T_F=1/2$ are the $SU(N)$ colour factors and n_f is the number of flavours. The "plus" functions appearing in the above results are the distributions which satisfy the following equation

$$
\int_0^1 dz\; f_+(z)\; g(z) \;=\; \int_0^1 dz\; f(z)\Big(g(z)-g(1)\Big),
$$

where

$$
f_+(z) \;=\; \left(\frac{\ln^i(1-z)}{1-z}\right)_+, \qquad i=0,1
$$

and $g(z)$ is any well behaved function in the region $0\le z\le 1$.

In Eqs. (2.3) and (2.4) the term $(1-3\cos^2\theta^*)$ corresponds to the interference between the SM and GR and within the SM interference between γ and Z diagrams. Though this combination is even in $\cos\theta^*$ it vanishes in the angular integrated cross section and also does not contribute to the forward-backward asymmetry A_{FB}. Hence the un-integrated cross section is very useful to study this contribution to the interference effect in the Drell-Yan process.

We present below the angular distribution which is "odd" in $\cos\theta^*$:

$$
\begin{aligned}
2S\,\frac{d\sigma_o^{P_1P_2}}{dQ^2 d\cos\theta^*} &= \sum_q \delta\mathcal{F}_{SM,q}\int_0^1 dx_1\int_0^1 dx_2\int_0^1 dz\;\delta(\tau-zx_1x_2)\\
&\times\Bigg[\delta H_{q\bar q}(x_1,x_2,\mu_F^2)\Big(\delta\Delta_{q\bar q}^{(0),\gamma Z}(z,Q^2,\mu_F^2)+a_s\delta\Delta_{q\bar q}^{(1),\gamma Z}(z,Q^2,\mu_F^2)\Big)\\
&+\delta H_{qg}(x_1,x_2,\mu_F^2)\Big(a_s\delta\Delta_{qg}^{(1),\gamma Z}(z,\mu_F^2)\Big)\\
&+\delta H_{gq}(x_1,x_2,\mu_F^2)\Big(a_s\delta\Delta_{gq}^{(1),\gamma Z}(z,\mu_F^2)\Big)\Bigg]\\
&+\sum_q \delta\mathcal{F}_{SMGR,q}\int_0^1 dx_1\int_0^1 dx_2\int_0^1 dz\;\delta(\tau-zx_1x_2)\\
&\times\Bigg[\delta H_{q\bar q}(x_1,x_2,\mu_F^2)\Big(\delta\Delta_{q\bar q}^{(0),G\gamma/Z}(z,Q^2,\mu_F^2)+a_s\delta\Delta_{q\bar q}^{(1),G\gamma/Z}(z,Q^2,\mu_F^2)\Big)\\
&+\delta H_{qg}(x_1,x_2,\mu_F^2)\Big(a_s\delta\Delta_{qg}^{(1),G\gamma/Z}(z,\mu_F^2)\Big)\\
&+\delta H_{gq}(x_1,x_2,\mu_F^2)\Big)\Big(a_s\delta\Delta_{gq}^{(1),G\gamma/Z}(z,\mu_F^2)\Big)\Bigg]. \qquad (2.5)
\end{aligned}
$$

The constants $\delta\mathcal{F}_{SM,q}, \delta\mathcal{F}_{SMGR,q}$ are given by

$$
\begin{aligned}
\delta\mathcal{F}_{SM,q} &= 2\alpha^2\Bigg[\frac{(Q^2-M_Z^2)}{((Q^2-M_Z^2)^2+M_Z^2\Gamma_Z^2)\,c_w^2 s_w^2}Q_qQ_eg_q^Ag_e^A\\
&+\frac{2Q^2}{((Q^2-M_Z^2)^2+M_Z^2\Gamma_Z^2)\,c_w^4 s_w^4}g_q^Vg_e^Vg_q^Ag_e^A\Bigg], \qquad (2.6)\\
\delta\mathcal{F}_{SMGR,q} &= \frac{\alpha\kappa^2Q^2}{4\pi}|\mathcal{D}(Q^2)|\Bigg[Q_qQ_e+\frac{Q^2(Q^2-M_Z^2)}{((Q^2-M_Z^2)^2+M_Z^2\Gamma_Z^2)\,c_w^2 s_w^2}g_q^Vg_e^V\Bigg]. \qquad (2.7)
\end{aligned}
$$

The renormalised incoming partonic fluxes are defined by

$$
\begin{aligned}
\delta H_{q\bar q}(x_1,x_2,\mu_F^2) &= f_q^{P_1}(x_1,\mu_F^2)\,f_{\bar q}^{P_2}(x_2,\mu_F^2)-f_{\bar q}^{P_1}(x_1,\mu_F^2)\,f_q^{P_2}(x_2,\mu_F^2),\\
\delta H_{gq}(x_1,x_2,\mu_F^2) &= f_g^{P_1}(x_1,\mu_F^2)\,\Big(f_q^{P_2}(x_2,\mu_F^2)-f_{\bar q}^{P_2}(x_2,\mu_F^2)\Big),
\end{aligned}
$$

$$\delta H_{qg}(x_1,x_2,\mu_F^2) \;=\; \delta H_{gq}(x_2,x_1,\mu_F^2)\,. \tag{2.8}$$

The LO coefficient functions corresponding to Eq. (2.5) are

$$\begin{aligned}
\delta\Delta_{q\bar{q}}^{(0),\gamma Z} &= \frac{2\pi}{N}\delta(1-z)\Big[\cos\theta^*\Big]\,,\\
\delta\Delta_{q\bar{q}}^{(0),G\gamma/Z} &= \frac{\pi}{8N}\delta(1-z)\Big[2\cos^3\theta^*\Big]\,.
\end{aligned} \tag{2.9}$$

The NLO contributions are given by

$$\begin{aligned}
\delta\Delta_{q\bar{q}}^{(1)\gamma Z} &= \frac{2\pi}{N}C_F\Bigg[\Big(8+8z-\frac{8}{1-z}\Big)\log(z)+\Big(-8-8z\Big)\log(1-z)\\
&\quad +16\left(\frac{\log(1-z)}{1-z}\right)_+ +\Big(-4-4z+\frac{8}{(1-z)_+}+6\delta(1-z)\Big)\log\left(\frac{Q^2}{\mu_F^2}\right)\\
&\quad +8\zeta(2)\delta(1-z)+4-4z-16\delta(1-z)\Bigg]\cos\theta^*\,,\\
\delta\Delta_{qg}^{(1)\gamma Z} &= \frac{2\pi}{N}T_F\Bigg[\Big(2-4z^2\Big)\log(z)+\Big(4-8z+8z^2\Big)\log(1-z)\\
&\quad +\Big(2-4z+4z^2\Big)\log\left(\frac{Q^2}{\mu_F^2}\right)+1+6z-7z^2\Bigg]\cos\theta^*\,,\\
\delta\Delta_{gq}^{(1)\gamma Z} &= \frac{2\pi}{N}T_F\Bigg[\Big(2-4z+12z^2\Big)\log(z)+\Big(-4+8z-8z^2\Big)\log(1-z)\\
&\quad +\Big(-2+4z-4z^2\Big)\log\left(\frac{Q^2}{\mu_F^2}\right)+1-2z+z^2\Bigg]\cos\theta^*\,,\\
\delta\Delta_{q\bar{q}}^{(1)G\gamma/Z} &= \frac{\pi}{8N}C_F\Bigg\{\Bigg[-\frac{16}{1-z}\log(z)+\Big(-16-16z\Big)\log(1-z)\\
&\quad +32\left(\frac{\log(1-z)}{1-z}\right)_+ +\Big(-8-8z+\frac{16}{(1-z)_+}+12\delta(1-z)\Big)\log\left(\frac{Q^2}{\mu_F^2}\right)\\
&\quad +16\zeta(2)\delta(1-z)-48+48z-36\delta(1-z)\Bigg]\cos^3\theta^*
\end{aligned}$$

$$
\begin{aligned}
&+\Big[24-24z\Big]\cos\theta^*\Big\}\,,\\
\delta\Delta_{qg}^{(1)G\gamma/Z} &= \frac{\pi}{8N}T_F\Big\{\Big[\Big(-12-24z-8z^2\Big)\log(z)+\Big(8-16z+16z^2\Big)\log(1-z)\\
&+\Big(4-8z+8z^2\Big)\log\left(\frac{Q^2}{\mu_F^2}\right)-38+52z-14z^2\Big]\cos^3\theta^*\\
&+\Big[24z\log(z)+24-24z\Big]\cos\theta^*\Big\}\,,\\
\delta\Delta_{gq}^{(1)G\gamma/Z} &= \frac{\pi}{8N}T_F\Big\{\Big[\Big(36+72z+24z^2\Big)\log(z)+\Big(-8+16z-16z^2\Big)\log(1-z)\\
&+\Big(-4+8z-8z^2\Big)\log\left(\frac{Q^2}{\mu_F^2}\right)+98-100z+2z^2\Big]\cos^3\theta^*\\
&+\Big[-48z\log(z)-48+48z\Big]\cos\theta^*\Big\}\,. \qquad (2.10)
\end{aligned}
$$

These coefficient functions Eq. (2.9) and (2.10), which are odd in $\cos\theta^*$, are due to the interference of γ and Z in SM and between SM and GR in the full theory. Note that the $q \to \bar{q}$ in the qg subprocess leads to a negative sign which has been taken care of in the renormalised parton fluxes Eq. (2.8). A_{FB} picks up this odd parts which contributes to the interference terms. To NLO the A_{FB} coefficient functions have been evaluated in [8] ¶ and the effects analysed for the ADD case. In the next section, the impact of the NLO-QCD correction derived in this section is discussed.

¶In [8] the last three equations of Eq. (6.11), the RHS should read $\Delta_{ab}^{(1)\gamma/Z}$.

3 Discussions

In this section, the effect of the NLO QCD corrections on the angular distribution of lepton pair are presented. We present these distributions for the LHC ($\sqrt{S} = 14\,\mathrm{TeV}$) and Run II of Tevatron ($\sqrt{S} = 1.96\,\mathrm{TeV}$) for typical values of ADD and RS model parameters. The effort here is mainly to emphasise the impact of QCD correction on the bounds rather than to extract bounds on M_S.

For ADD model, we choose the parameters $M_S = 2$ TeV and $d = 3$. For RS we choose $c_0 = 0.01$, $M_1 = 1.5$ TeV(for LHC) and $M_1 = 700$ GeV(for Tevatron). The SM parameters which enter our analysis are $\alpha = 1/137.03604$, $M_Z = 91.1876$ GeV, $\Gamma_Z = 2.4952$ GeV and $\sin^2\theta_W = 0.227$. For the parton density sets, we adopt in leading order, the MRST 2001 LO ($\Lambda = 0.1670$ GeV) and in next-to-leading order, the MRST 2001 NLO ($\Lambda = 0.2390$ GeV). The renormalisation scale μ_R and factorisation scale μ_F are taken to be equal to Q unless mentioned otherwise.

For the coefficient functions which are even in $\cos\theta^*$, the parton density combinations are even under the interchange of x_1 and x_2, while for the odd terms in $\cos\theta^*$, the parton density combinations are odd under this exchange. Hence, the quark-antiquark initiated contributions from these odd terms to LHC cross sections are zero, but small contribution comes from quark-gluon initiated processes. This is not the case for Tevatron.

In the SM part, at LO level, the quark-antiquark initiated processes behave as $1 + \cos^2\theta^*$ for pure γ and Z intermediate states, and as $\cos\theta^*$ for γZ interference terms. In the Gravity part, at LO, gluon-gluon initiated process is of the form $1 - \cos^4\theta^*$, quark-antiquark process is of the form $1 - 3\cos^2\theta^* + 4\cos^4\theta^*$. The interference between SM and GR always behaves as $\cos\theta^*$, $\cos^3\theta^*$ and $1 - 3\cos^2\theta^*$. At NLO, quark-gluon initiated processes contribute to both SM, GR and the interference terms.

We first discuss the phenomenology at LHC using ADD model. In Fig. 1a, we

plot the angular distribution at $Q = 700$ GeV with NLO corrected cross sections. We find that the gravity contribution is large compared to that of SM. Since the gluon flux is large at LHC, the gluon-gluon initiated subprocess dominates over the rest. Also, the interference between SM and Gravity is negligible over the entire range of $\cos\theta^*$ at this $Q = 700$ GeV. In the Fig. 1b, we have plotted the K-factor at LHC. In general K-factor is defined as

$$K = \left[\frac{d\sigma^I_{LO}(Q,\cos\theta^*)}{dQd\cos\theta^*}\right]^{-1}\left[\frac{d\sigma^I_{NLO}(Q,\cos\theta^*)}{dQd\cos\theta^*}\right] , \tag{3.1}$$

where $I = SM, TOT$, SM means Standard Model, TOT means sum of SM and Gravity contributions. Since the gluon-gluon initiated process dominates over the rest the K-factor is around 1.4 to 1.5 in the entire range of $\cos\theta^*$. In the Fig. 1c we have plotted the R-ratio in order to check whether the NLO results improve the scale uncertainty. Here we have chosen $\mu_R = \mu_F = \mu$ and we follow the same throughout our analysis. The R-ratio is defined as

$$R^I_{LO} = \left[\frac{d\sigma^I_{LO}(\mu=\mu_0))}{dQd\cos\theta^*}\right]^{-1}\left[\frac{d\sigma^I_{LO}(\mu))}{dQd\cos\theta^*}\right]_{Q=700\ GeV} , \tag{3.2}$$

$$R_{NLO} = \left[\frac{d\sigma^I_{NLO}(\mu=\mu_0))}{dQd\cos\theta^*}\right]^{-1}\left[\frac{d\sigma^I_{NLO}(\mu))}{dQd\cos\theta^*}\right]_{Q=700\ GeV} . \tag{3.3}$$

We have chosen $\theta^* = 45^0$ for the plot. As we can see the NLO results improve the scale uncertainty.

Let us now repeat the similar study for the RS model at LHC energies. In the Fig. 2a, we have plotted the angular distribution at first resonance $M_1 = 1.5$ TeV and $c_0 = 0.01$. We find that the gravity contribution is well above the standard model one. In particular, the gluon-gluon initiated contribution is the dominant one. Since the SM and interference contributions are of the same order and are extremely small due to large Q which is 1.5 TeV, the total contribution is purely due to the gluon-gluon initiated process. Unlike the ADD case (see Fig. 1a), the total contribution

mainly comes from the gravity mediated process at the first resonance. In Fig. 2b, we have plotted the K-factor defined in Eq. (3.1) at the first resonance. Because of this, the dominant contribution comes from the gravity mediated processes. Since $Q = 1.5$ TeV, both quark-antiquark as well as the gluon initiated processes contribute at the same level because their partonic fluxes are comparable at this energy. The shape of the K-factor in Fig. 1b looks different from Fig. 2b because at $Q = 0.7$ TeV, only gluon initiated process dominates. In Fig. 2c, we have plotted the R-ratio defined in Eq. (3.2, 3.3) for RS resonance $M_1 = 1.5$ TeV, $c_0 = 0.01$ at $\theta^* = 45^0$. From the plot it is clear that the NLO corrections improve the scale uncertainty.

Next we discuss the phenomenology at Tevatron. We start with ADD for the parameters $M_S = 2$ TeV, $d = 3$ and $Q = 400$ GeV. In Fig. 3a we have plotted angular distribution with NLO results. We find that the SM dominates over the rest. In Tevatron, both the even and odd in $\cos\theta^*$ contribute significantly unlike in the LHC. This leads to the asymmetry in the angular distribution as shown in Fig. 3a at Tevatron. At $Q = 400$ GeV the dominant contribution at Tevatron is from SM. In Fig. 3b, we have plotted the K-factor at $Q = 400$ GeV. Since it is the quark-antiquark initiated process that dominates, the K-factor is similar to the SM value which is around 1.3. Fig. 3c shows the sensitivity of the results to the scale variation. As expected NLO improves the result.

We now study the phenomenology at Tevatron in the case of RS model. We choose the RS model parameters $M_1 = 700$ GeV and $c_0 = 0.01$ which are not excluded by the recent searches by DØ[13]. In Fig. 4a, we have plotted the angular distribution at the first resonance using NLO corrected cross sections. Being in the resonance region, gravity mediated process dominates over the SM. At $Q = 700$ GeV, the quark initiated processes contribute significantly, as the $q\bar{q}$ flux dominates. In Fig. 4b, we have plotted the K-factor at $Q = 700$ GeV. Since the quark initiated process dominates, the K-factor is close to the SM value. Fig. 4c shows the sensitiv-

ity of the results with respect to scale. One can easily notice that NLO gives reliable predictions.

In summary, we have computed the cross sections $d\sigma/dQ/d\cos\theta^*$ up to next to leading order in QCD. Along with the standard model results, we have presented the contributions from all the subprocesses that are due to the graviton in the context of TeV-scale gravity models. Our main conclusion is that the NLO QCD corrections are very significant at the LHC because of the large incident gluon flux. At the Tevatron where the gluon flux is small, the NLO effects are moderate for ADD and RS in the resonance region. But, significantly, at both the colliders the inclusion of the NLO QCD corrections help stabilise the cross-section with respect to scale variations. The extraction of bounds from both the colliders will, therefore, require the inclusion of these NLO QCD corrections.

Acknowledgments:
The work of PM is part of a project (IFCPAR Project No. 2904-2) on 'Brane-World Phenomenology' supported by the Indo-French Centre for the Promotion of Advanced Research, New Delhi, India. We thank S. Raychaudhuri for providing the code that evaluates the RS KK mode sum in the propagator.

Figure Caption

Figure 1. (a) The double differential cross section $d\sigma/dQ/d\cos\theta^*$ is plotted as a function of $\cos\theta^*$ for $Q = 700$ GeV at LHC. The typical ADD parameters chosen are $M_S = 2$ TeV, $d = 3$. (b) The corresponding K-factor for $\cos\theta^*$ distribution SM and SM plus gravity (TOT). (c) Scale variation at LO and NLO as defined in Eq. (3.2), (3.3) for $Q = 700$ GeV and $\theta^* = 45^0$.

Figure 2. (a) The double differential cross section $d\sigma/dQ/d\cos\theta^*$ is plotted as a function of $\cos\theta^*$ for $Q = 1.5$ TeV at LHC. The RS model parameters are $M_1 = 1.5$ TeV and $c_0 = 0.01$. (b) The K-factor for the distribution in (a) is plotted for the $\cos\theta^*$ range [-1,1]. (c) The scale variation of the ratio R is plotted as a function of μ/μ_0 at the first RS KK resonance region and $\theta^* = 45^0$.

Figure 3. (a) For Tevatron energies, $d\sigma/dQ/d\cos\theta^*$ is plotted as a function of $\cos\theta^*$ at $Q = 400$ GeV for typical value of ADD parameters $M_S = 2$ TeV and $d = 3$. (b) The K-factor for $\cos\theta^*$ distribution for the same ADD parameters in (a) is plotted. (c) The variation of the R-ratio with respect to the scale μ/μ_0 for the ADD parameters in (a) at $\theta^* = 45^0$.

Figure 4. (a) The double differential cross section $d\sigma/dQ/d\cos\theta^*$ is plotted as a function of $\cos\theta^*$ for $Q = 700$ GeV at the Tevatron. RS parameters $M_1 = 700$ GeV and $c_0 = 0.01$. (b) The K-factor for the distribution in (a) is plotted for the $\cos\theta^*$ range. (c) The scale variation of the ratio R is plotted as a function of μ/μ_0 for $\theta^* = 45^0$ and $Q = 700$ GeV.

References

[1] N. Arkani-Hamed, S. Dimopoulos and G. Dvali, *Phys. Lett.* **B249** (1998) 263; I. Antoniadis, N. Arkani-Hamed, S. Dimopoulos and G. Dvali, *Phys. Lett.* **B436** (1998) 257.

[2] L. Randall and R. Sundrum, *Phys. Rev. Lett.* **83** (1999) 3370.

[3] C. D. Hoyle *et. al*, *Phys. Rev.* **D70** (2004) 042004.

[4] G. F. Giudice, R. Rattazzi and J. D. Wells, *Nucl. Phys.* **B544** (1999) 3.

[5] T. Han, J. D. Lykken and R-J. Zhang, *Phys. Rev.* **D59** (1999) 105006.

[6] W.D. Goldberger and M.B. Wise, *Phys. Rev. Lett.* **83** (1999) 4922; *Phys.Lett.* **B475** (2000) 275.

[7] Prakash Mathews, V. Ravindran and K. Sridhar, *JHEP* **0408** (2004) 048.

[8] Prakash Mathews, V. Ravindran, K. Sridhar and W.L. van Neerven *Nucl. Phys.* **B713** (2005) 333.

[9] Prakash Mathews, V. Ravindran and K. Sridhar, *JHEP* **0510** (2005) 031.

[10] K. Cheung and G. Landsberg, *Phys. Rev.* **D62** (2000) 076003.

[11] V. M. Abazov *et. al.*, DØ Collaboration, *Phys. Rev. Lett.* **95** (2005) 161602.

[12] V. M. Abazov *et. al.*, DØ Collaboration, *Phys. Rev. Lett.* **86** (2001) 1156.

[13] V. M. Abazov *et. al.*, DØ Collaboration, *Phys. Rev. Lett.* **95** (2005) 091801.

[14] J. Kodaira and H. Yokoya, *Phys. Rev.* **D67** (2003) 074008.

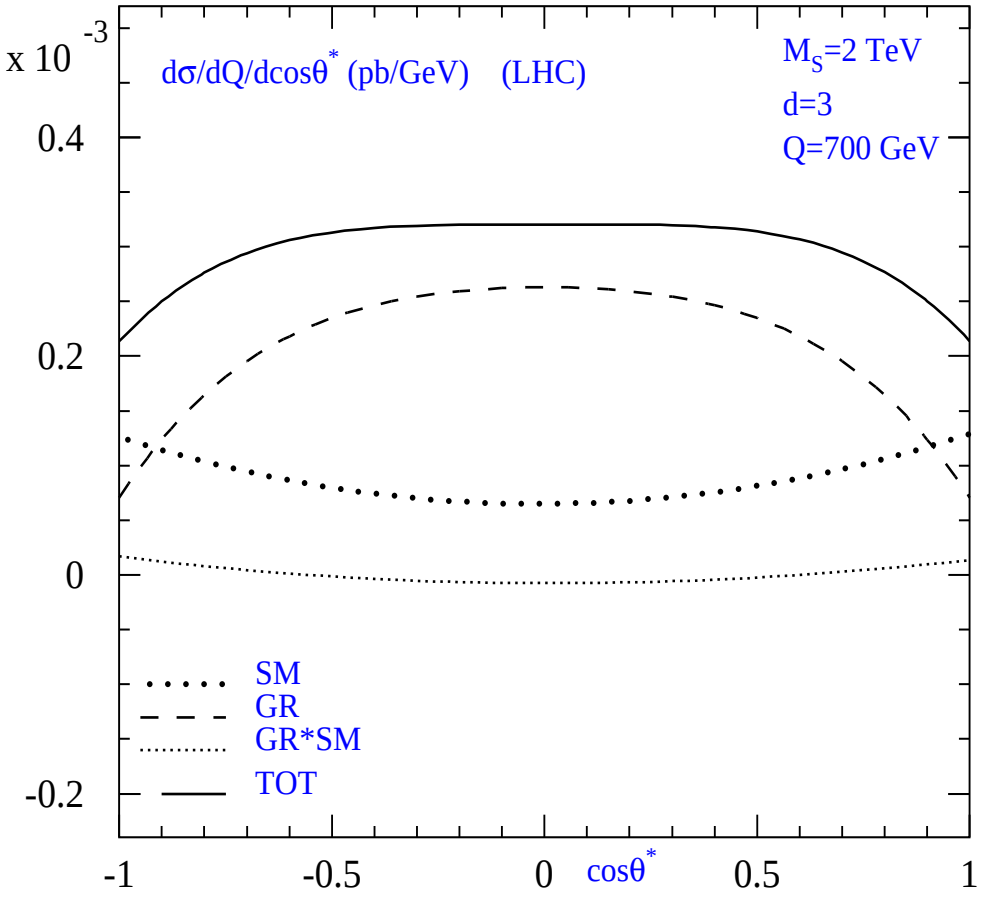
x 10 -3
dσ/dQ/dcosθ* (pb/GeV) (LHC)
M_S=2 TeV
d=3
Q=700 GeV
0.4
0.2
0
-0.2
SM
GR
GR*SM
TOT
-1
-0.5
0
cosθ*
0.5
1

Fig. 1a

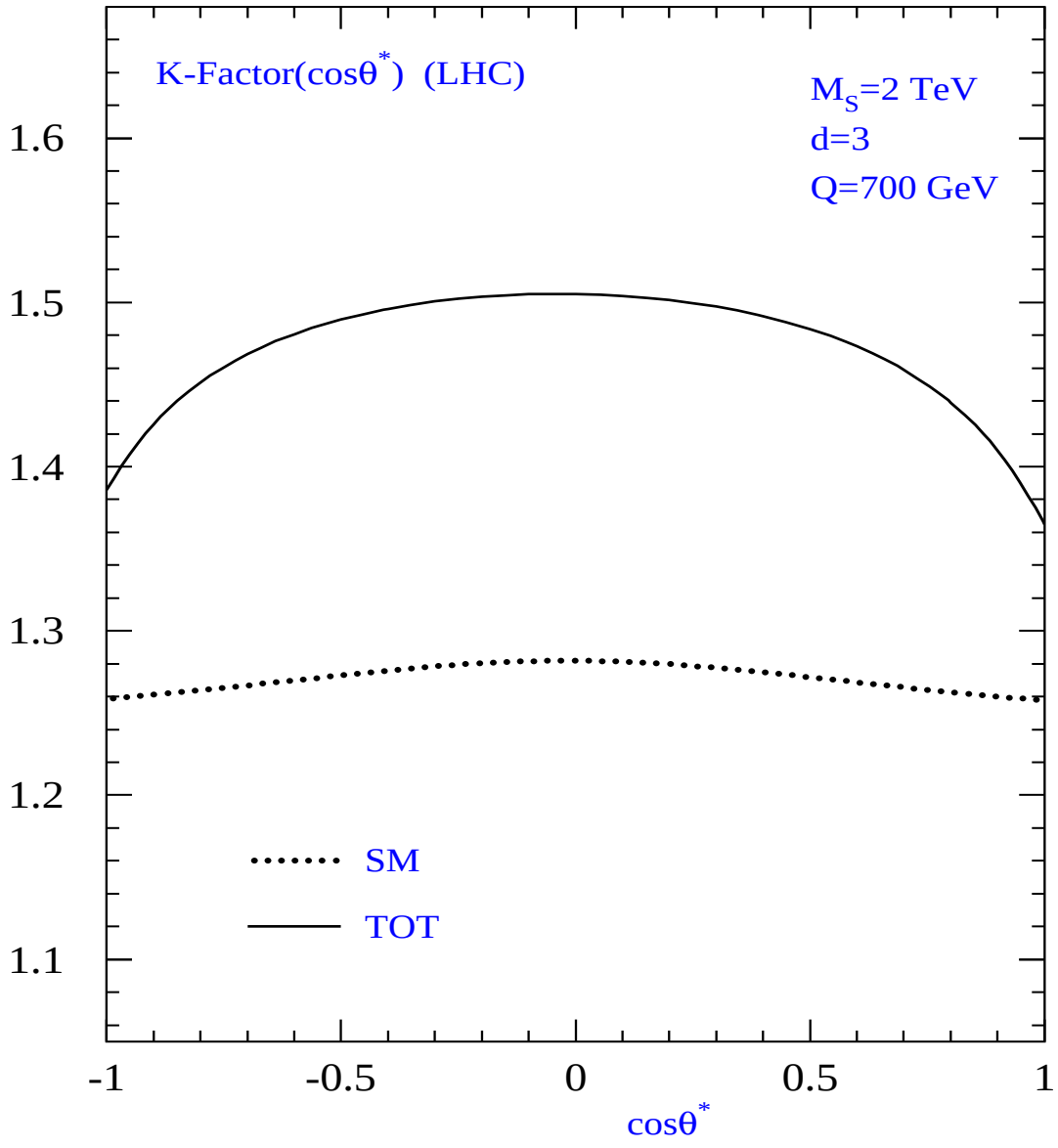
K-Factor(cosθ*) (LHC)
M_S=2 TeV
d=3
Q=700 GeV
1.6
1.5
1.4
1.3
1.2
1.1
SM
TOT
-1
-0.5
0
0.5
1
cosθ*

Fig. 1b

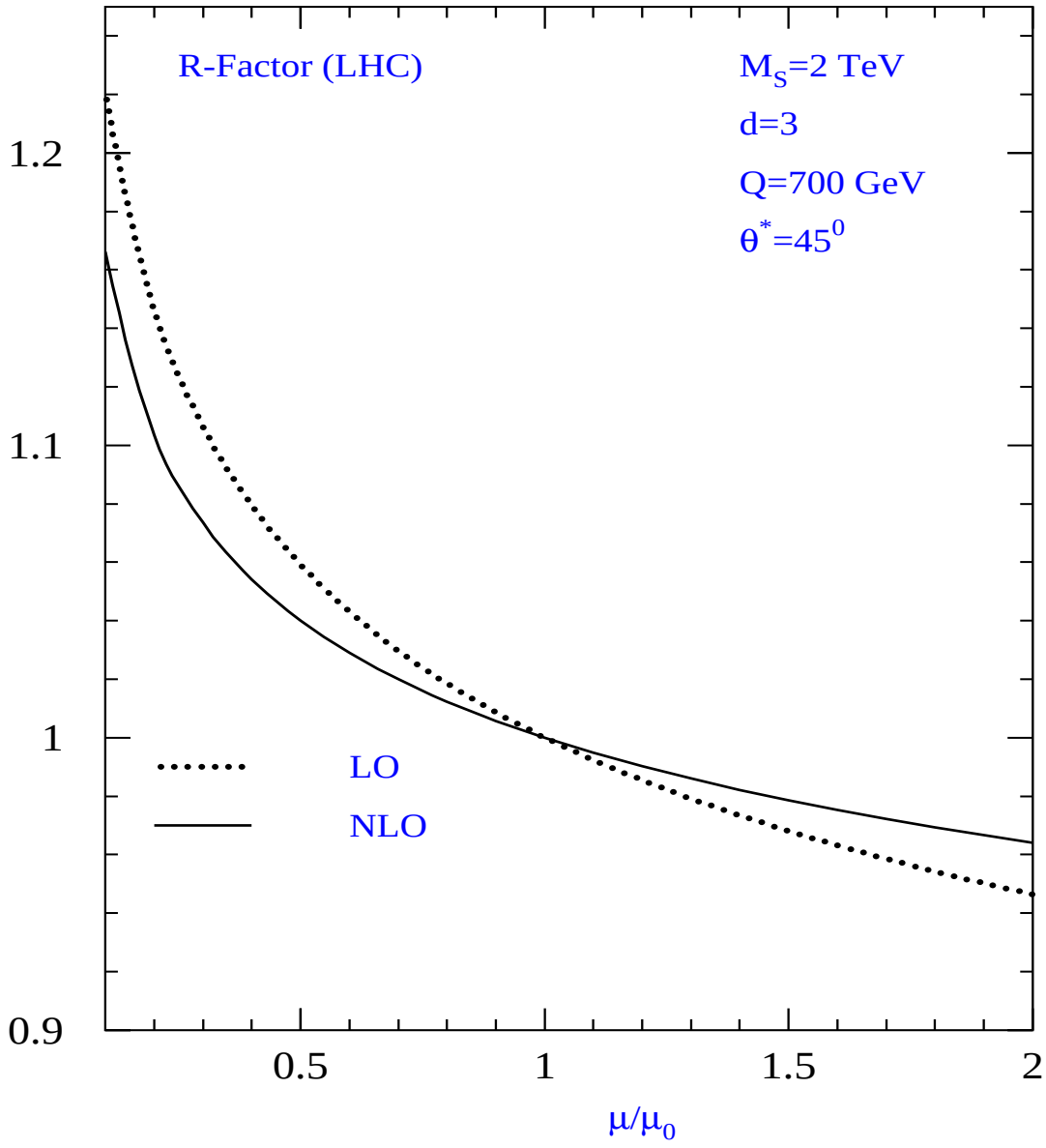
R-Factor (LHC)
M_S=2 TeV
d=3
Q=700 GeV
θ*=45^0
LO
NLO
1.2
1.1
1
0.9
0.5
1
1.5
2
μ/μ_0

Fig. 1c

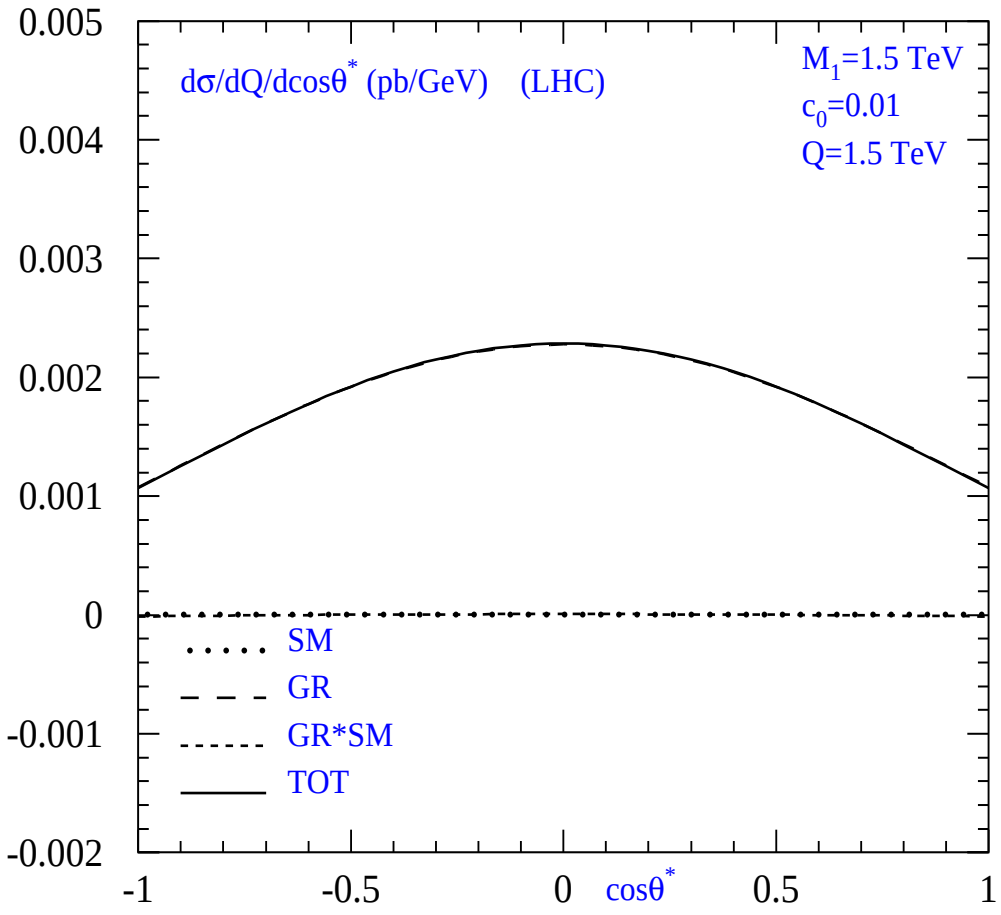
0.005
0.004
0.003
0.002
0.001
0
-0.001
-0.002
-1
-0.5
0
0.5
1
cosθ*
dσ/dQ/dcosθ* (pb/GeV) (LHC)
M1=1.5 TeV
c0=0.01
Q=1.5 TeV
SM
GR
GR*SM
TOT

Fig. 2a

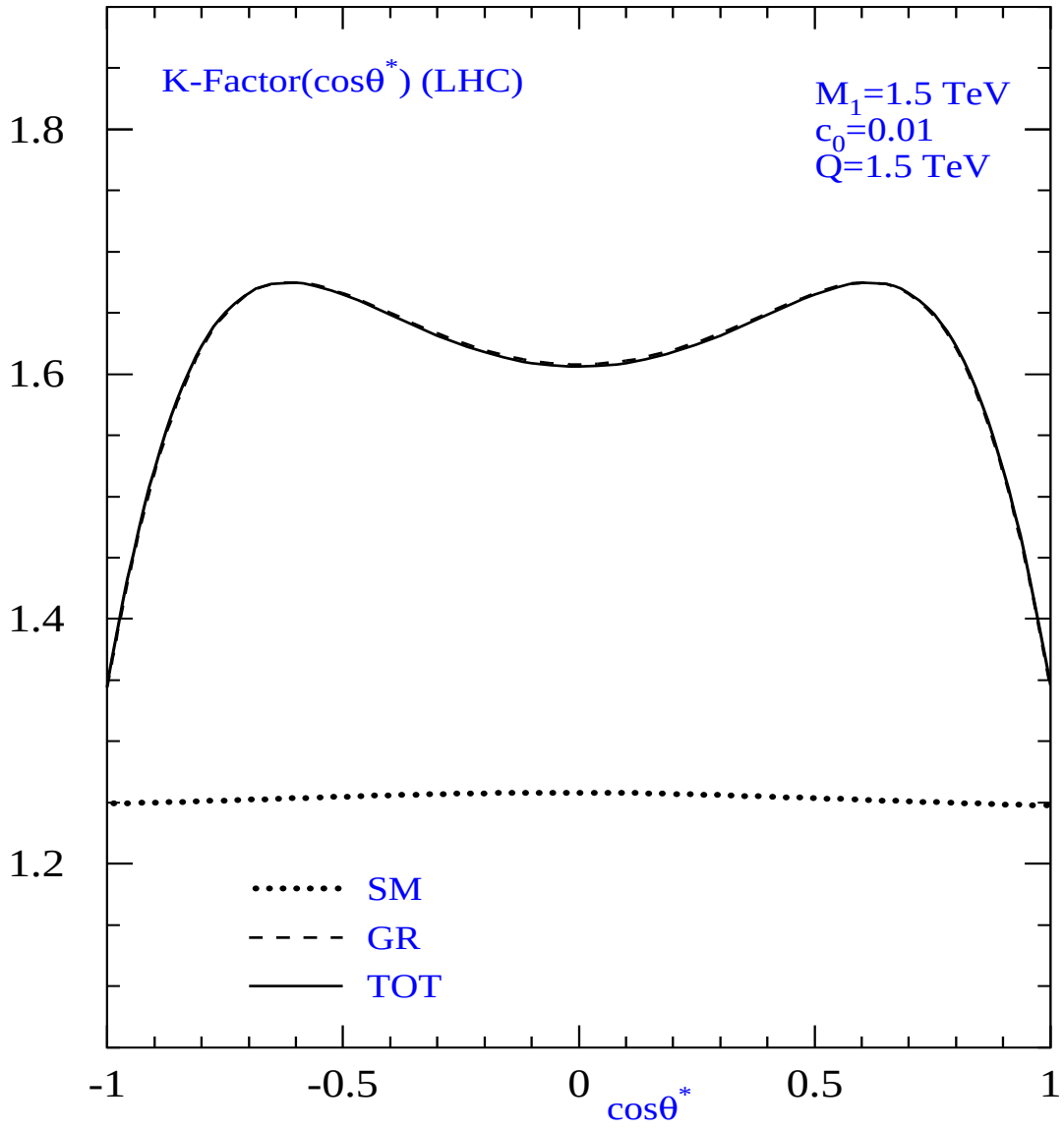
K-Factor(cosθ*) (LHC)
M1=1.5 TeV
c0=0.01
Q=1.5 TeV
1.8
1.6
1.4
1.2
SM
GR
TOT
-1
-0.5
0
0.5
1
cosθ*

Fig. 2b

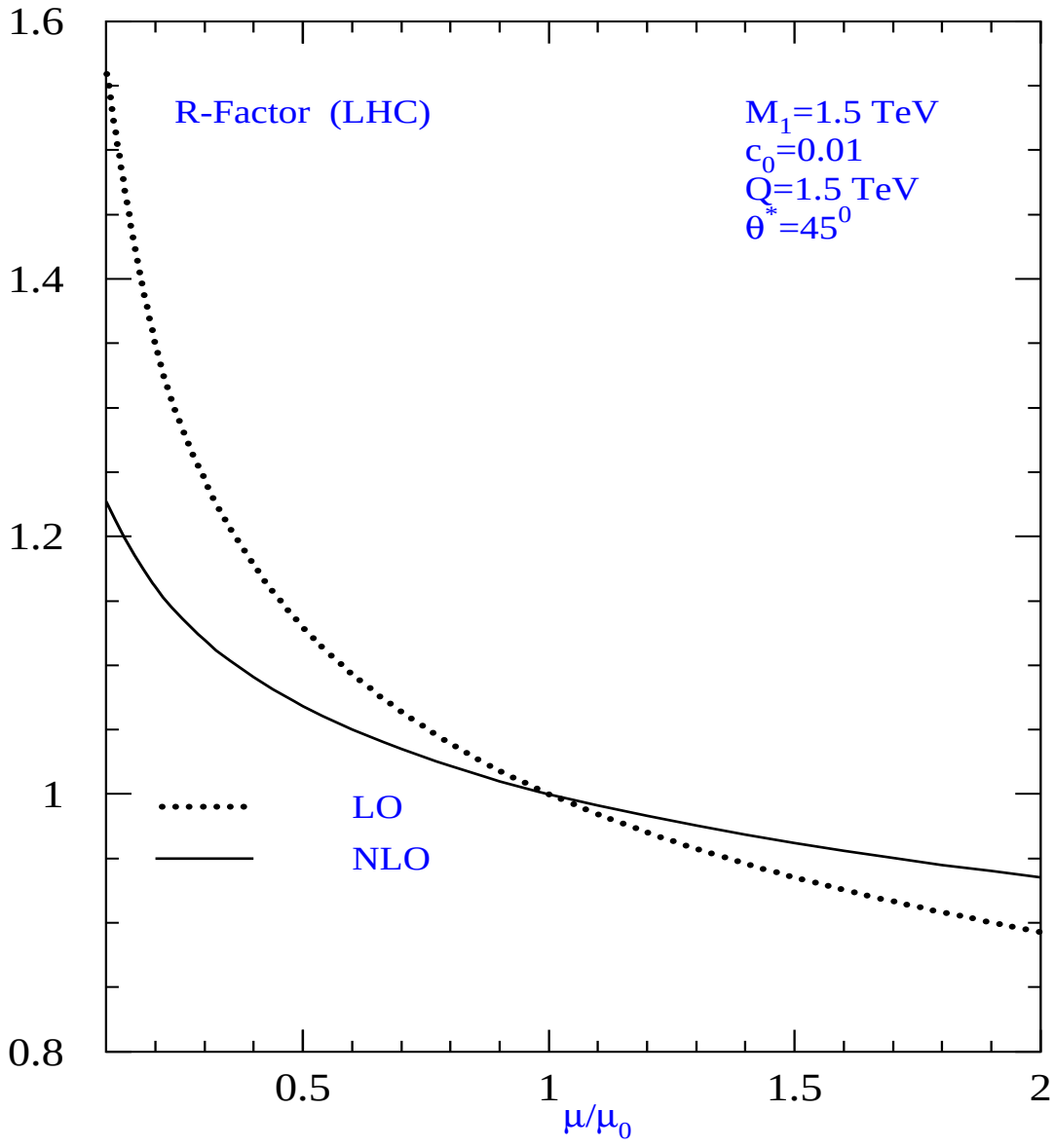
R-Factor (LHC)
M1=1.5 TeV
c0=0.01
Q=1.5 TeV
θ*=45^0
LO
NLO
1.6
1.4
1.2
1
0.8
0.5
1
1.5
2
μ/μ0

Fig. 2c

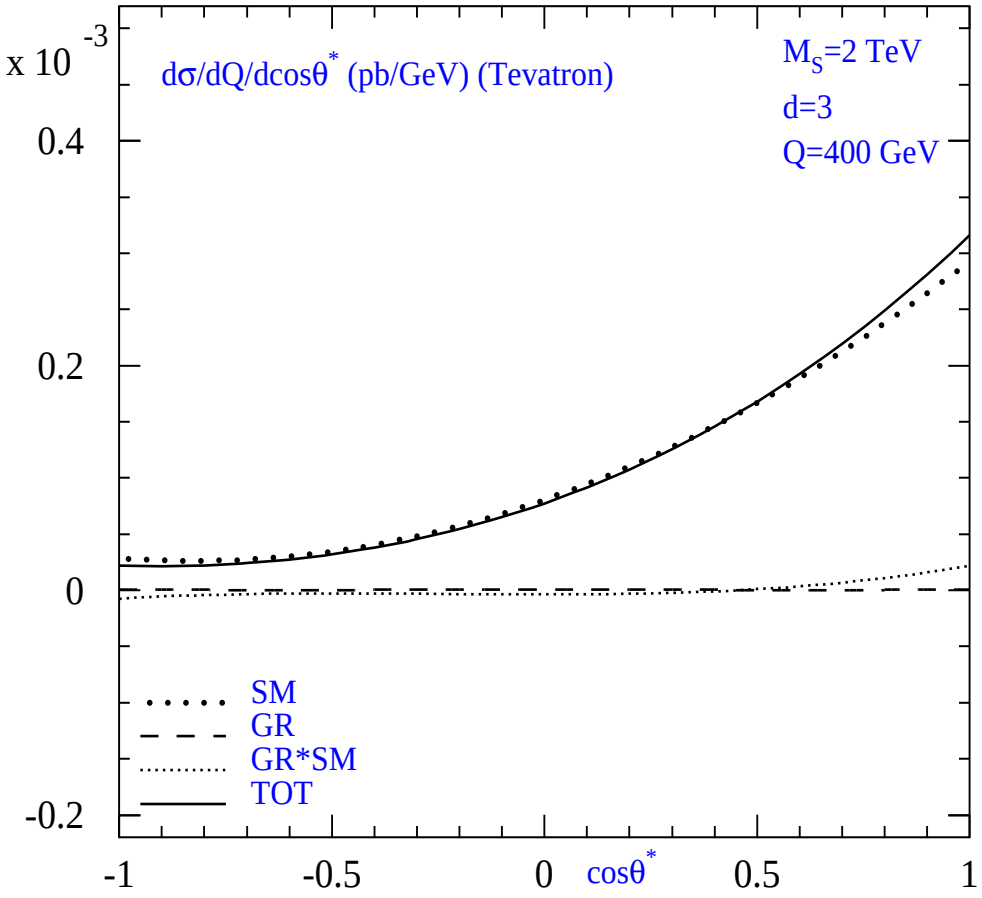
x 10 -3
dσ/dQ/dcosθ* (pb/GeV) (Tevatron)
M_S=2 TeV
d=3
Q=400 GeV
0.4
0.2
0
-0.2
SM
GR
GR*SM
TOT
-1
-0.5
0
cosθ*
0.5
1

Fig. 3a

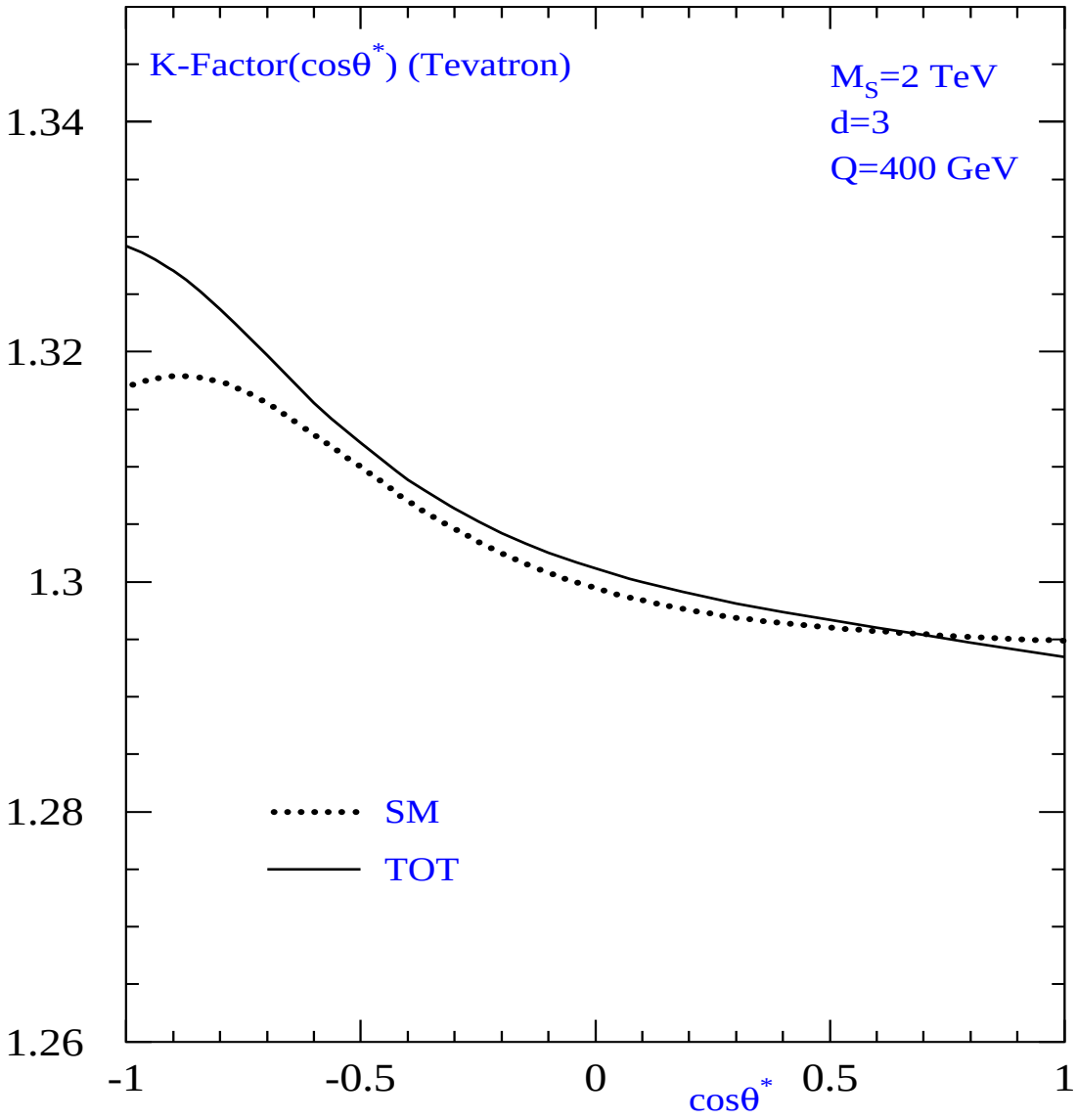
K-Factor(cosθ*) (Tevatron)
M_S=2 TeV
d=3
Q=400 GeV
1.34
1.32
1.3
1.28
1.26
SM
TOT
-1
-0.5
0
0.5
1
cosθ*

Fig. 3b

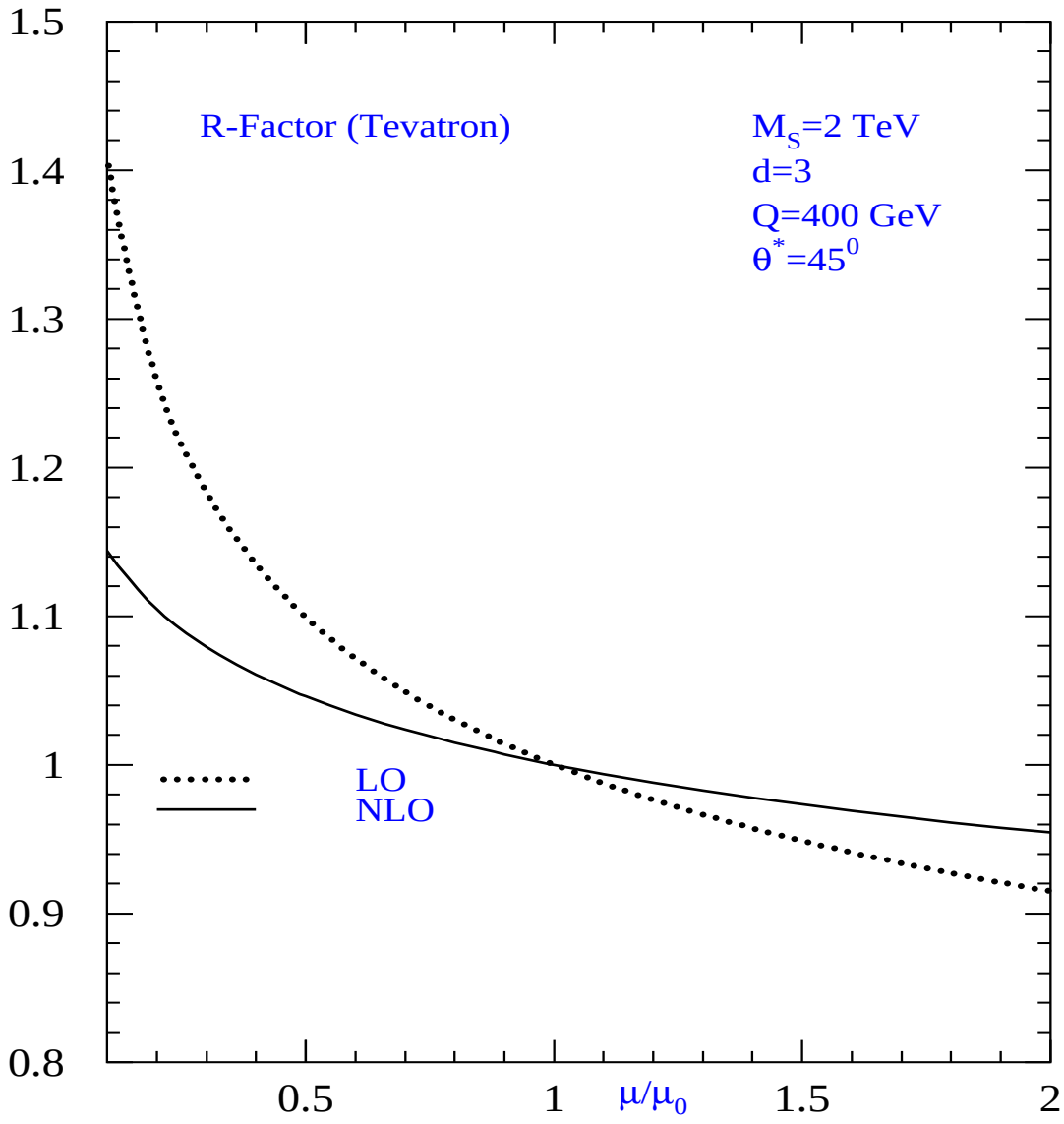
R-Factor (Tevatron)
M_S=2 TeV
d=3
Q=400 GeV
$\theta^*=45^0$
LO
NLO
1.5
1.4
1.3
1.2
1.1
1
0.9
0.8
0.5
1
μ/μ_0
1.5
2

Fig. 3c

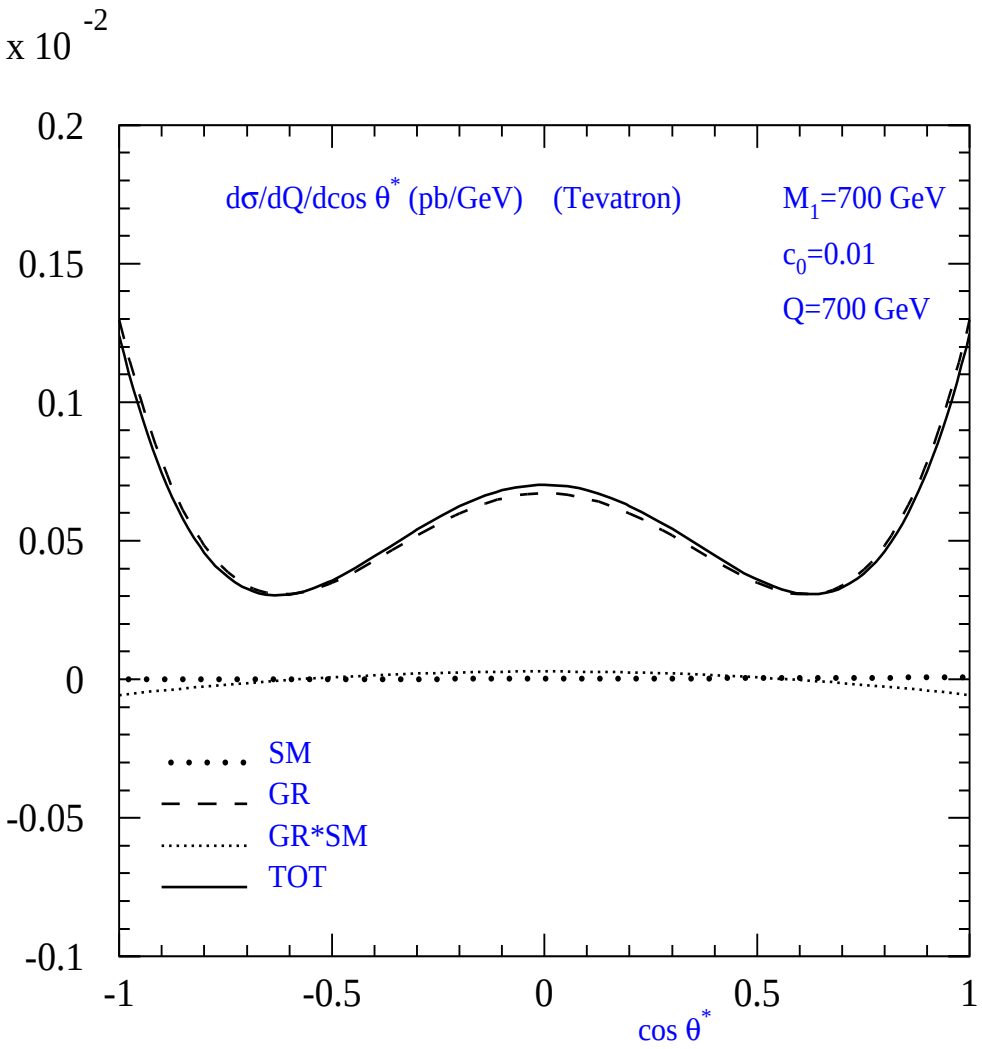
x 10 -2
0.2
0.15
0.1
0.05
0
-0.05
-0.1
dσ/dQ/dcos θ* (pb/GeV) (Tevatron)
M1=700 GeV
c0=0.01
Q=700 GeV
SM
GR
GR*SM
TOT
-1
-0.5
0
0.5
1
cos θ*

Fig. 4a

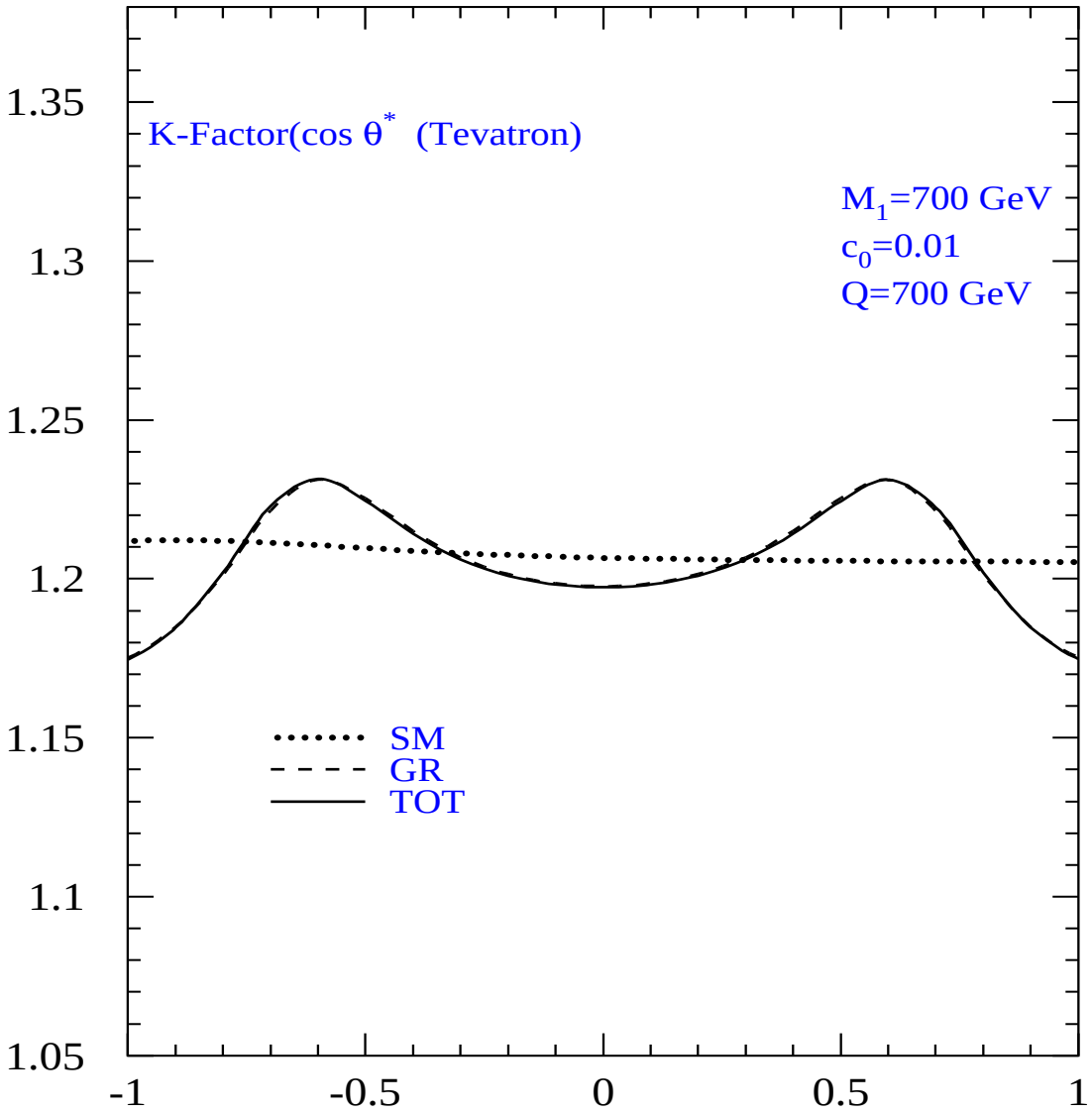
K-Factor(cos θ* (Tevatron)
M1=700 GeV
c0=0.01
Q=700 GeV
SM
GR
TOT
1.35
1.3
1.25
1.2
1.15
1.1
1.05
-1
-0.5
0
0.5
1

Fig. 4b

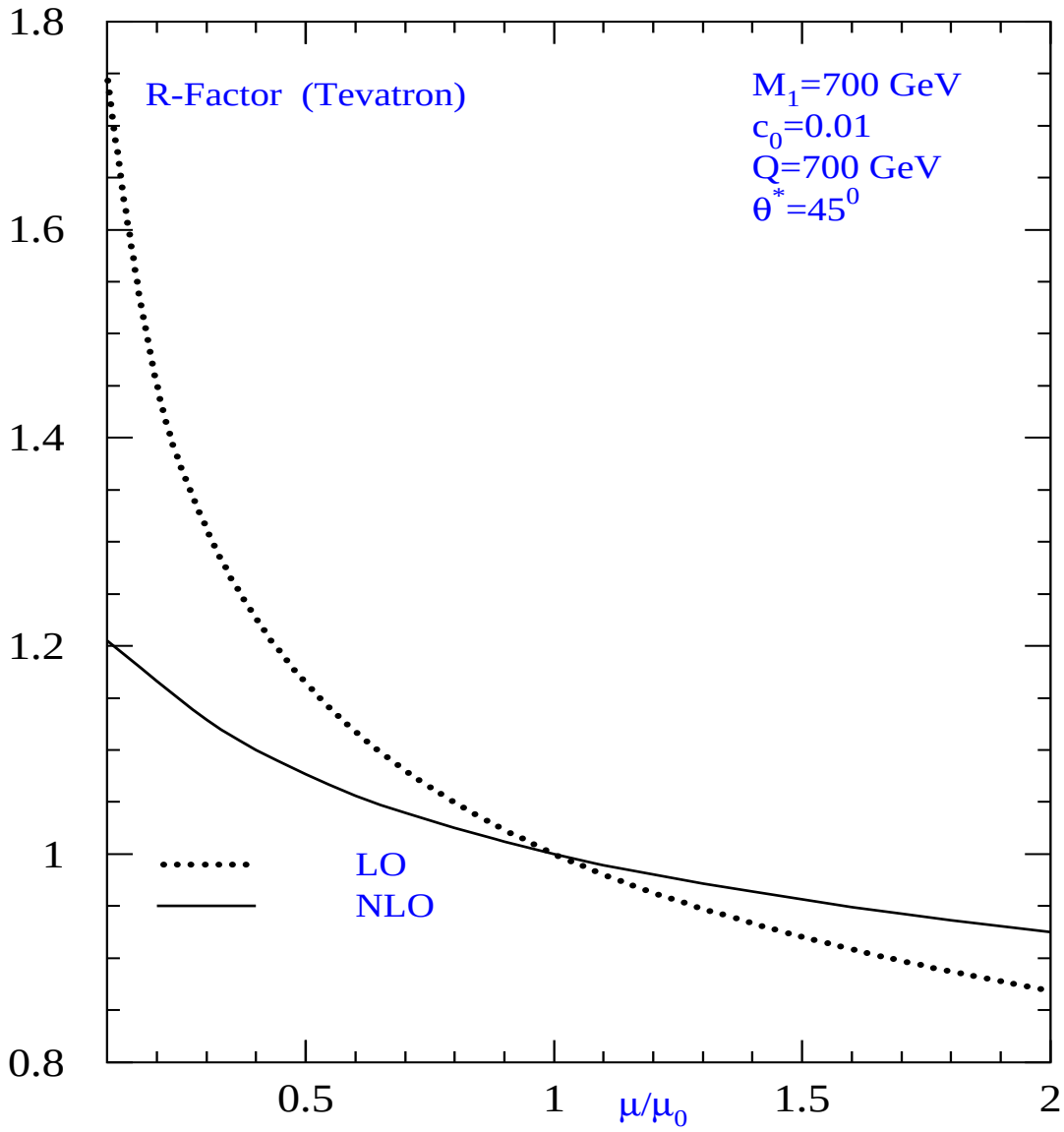
R-Factor (Tevatron)
M1=700 GeV
c0=0.01
Q=700 GeV
θ*=45^0
LO
NLO
1.8
1.6
1.4
1.2
1
0.8
0.5
1
1.5
2
μ/μ0

Fig. 4c